

Supplementary Information

Ultra-thin flexible paper of BNNT-CNF/ZnO ternary nanostructure for enhanced solid-state supercapacitor and piezoelectric response

Iqra Rabani^a, Ye-Jee park^a, Je-Won Lee^a, Muhammad Shoaib Tahir^a, Ajeet Kumar^b and Young-Soo Seo^{a*}

^aDepartment of Nanotechnology and Advanced Materials Engineering, Sejong University, Seoul 05006, Republic of Korea

^bSchool of Materials Science and Engineering, Yeungnam University, Gyeongsan 38541, Republic of Korea.

*Corresponding author E-mail: ysseo@sejong.ac.kr

Figure Content

S1.

Preparation of the ZnO nanoparticles

Figure S2 (a-c).

High-resolution O 1s x-ray photoelectron spectroscopy for the **(a)** pristine BNNT, **(b)** BNNT-ZnO hybrid and **(c)** BNNT-CNF/ZnO ternary nanostructure.

Figure S3 (a-d).

Cyclic Voltammetry (CV) curves for the **(a)** pristine BNNT, **(b)** pristine ZnO, **(c)** BNNT-CNF hybrid and **(d)** BNNT-ZnO hybrid under various scan rates ranging from 10 mV/s to 60 mV/s in three electrode measurements.

Figure S4 (a-d).

Galvanostatic charging-discharging curves for the **(a)** pristine BNNT, **(b)** pristine ZnO, **(c)** BNNT-CNF hybrid and **(d)** BNNT-ZnO hybrid under various scan rates ranging from 10 mV/s to 60 mV/s in three electrode measurements.

Figure S5.

Cycling stability test under 5000 GCD cycles for the pristine BNNT, pristine ZnO, BNNT-CNF, BNNT-ZnO hybrid and BNNT-CNF/ZnO ternary nanostructure under 20 A/g of current density in a three electrode measurements.

Figure S6.

CV curves of BNNT-ZnO hybrid under various scan rates ranging from 10 mV/s to 50 mV/s in two electrode measurements.

Figure S7.

CV curves of BNNT-CNF hybrid under various scan rates ranging from 10 mV/s to 50 mV/s in two electrode measurements.

- Figure S8.** CV curves of pristine ZnO under various scan rates ranging from 10 mV/s to 50 mV/s in two electrode measurements.
- Figure S9.** CV curves of pristine BNNT under various scan rates ranging from 10 mV/s to 50 mV/s in two electrode measurements.
- Figure S10.** GCD curves of BNNT-ZnO hybrid under various current densities ranging from 1 A/g to 10 A/g in two electrode measurements.
- Figure S11.** GCD curves of BNNT-CNF hybrid under various current densities ranging from 1 A/g to 10 A/g in two electrode measurements.
- Figure S12.** GCD curves of pristine ZnO under various current densities ranging from 1 A/g to 10 A/g in two electrode measurements.
- Figure S13.** GCD curves of pristine BNNT under various current densities ranging from 1 A/g to 10 A/g in two electrode measurements.
- Figure S14.** BNNT-CNF/ZnO ternary nanostructure paper performance such as **(a)** FESEM micrographs before cycling stability test, **(b)** after cycling stability (over 5000 cycles), and **(c)** XRD after cycling stability test. **(d)** Photo digital images for the BNNT-CNF/ZnO ternary nanostructure papers at different positions and **(e)** flexible symmetric supercapacitor device picture at different positions.
- Figure S15.** FESEM micrographs of the BNNT-CNF and BNNT-CNF/ZnO flexible paper.

Table S1. Comparative electrochemical performance of BNNT-CNF/ZnO in the three-electrode system with other previously reported materials.

Table S2. Comparative electrochemical performance of BNNT-CNF/ZnO in all solid state symmetric/Asymmetric supercapacitor devices with other previously reported materials.

References

S1. Preparation of the ZnO nanoparticles

Typically, Zinc acetate (2.6 wt%) and KOH (0.26 wt%) were each dispersed in methanol at 60 °C. The molar ratio of zinc acetate and KOH was fixed as 2:1. The KOH solution was added dropwise into the Zn (CH₃COO)₂.2H₂O solution under constant stirring for 1.5 h at 60 °C. Consequently, the solution mixture was permitted to cool slowly at ambient conditions, than the mixture was cleaned by using centrifugations (7000 rpm, 10 min) with the ethanol and deionized (DI) water. The final white precipitate was obtained and dried in a oven for overnight and the product was labelled as ZnO NP.

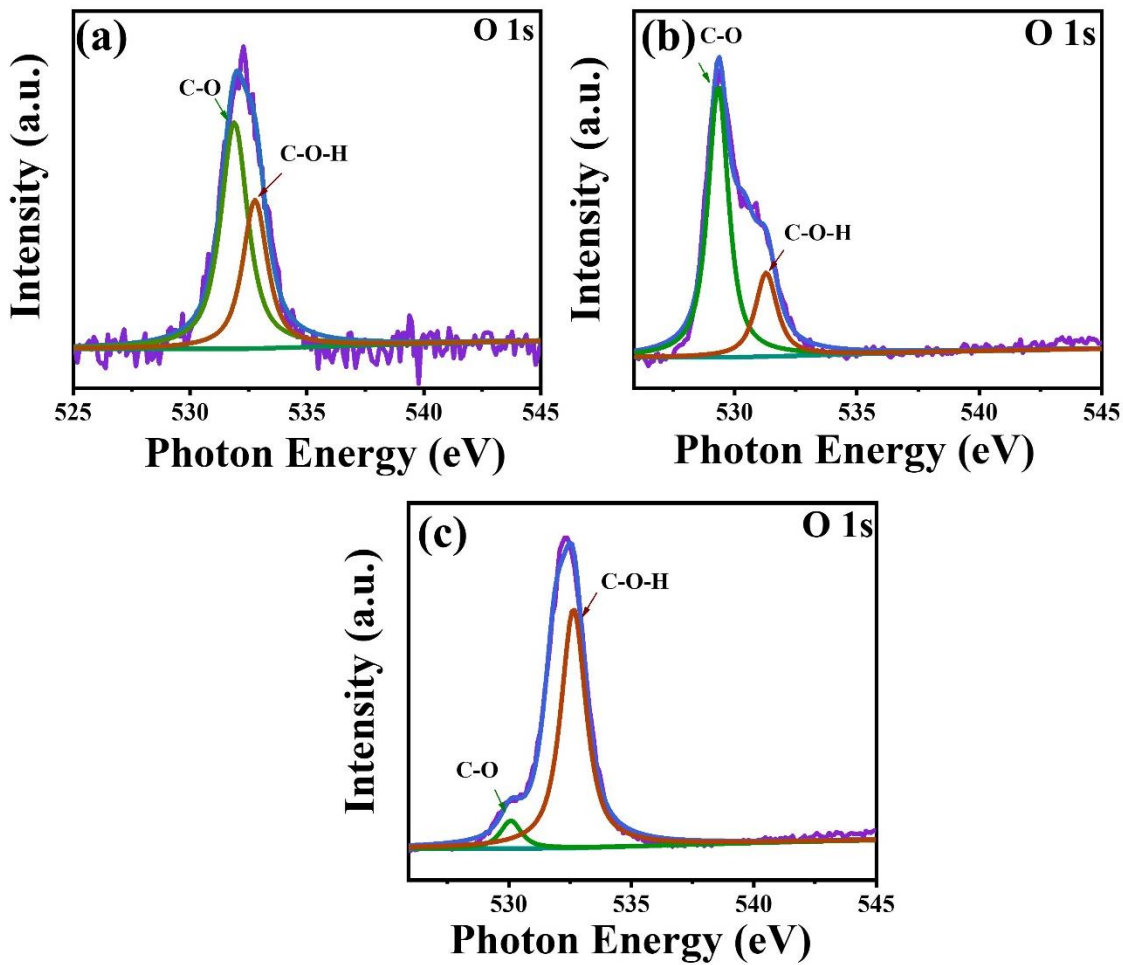


Figure S2 (a-c). High-resolution O 1s x-ray photoelectron spectroscopy for the (a) pristine BNNT, (b) BNNT-ZnO hybrid and (c) BNNT-CNF/ZnO ternary nanostructure.

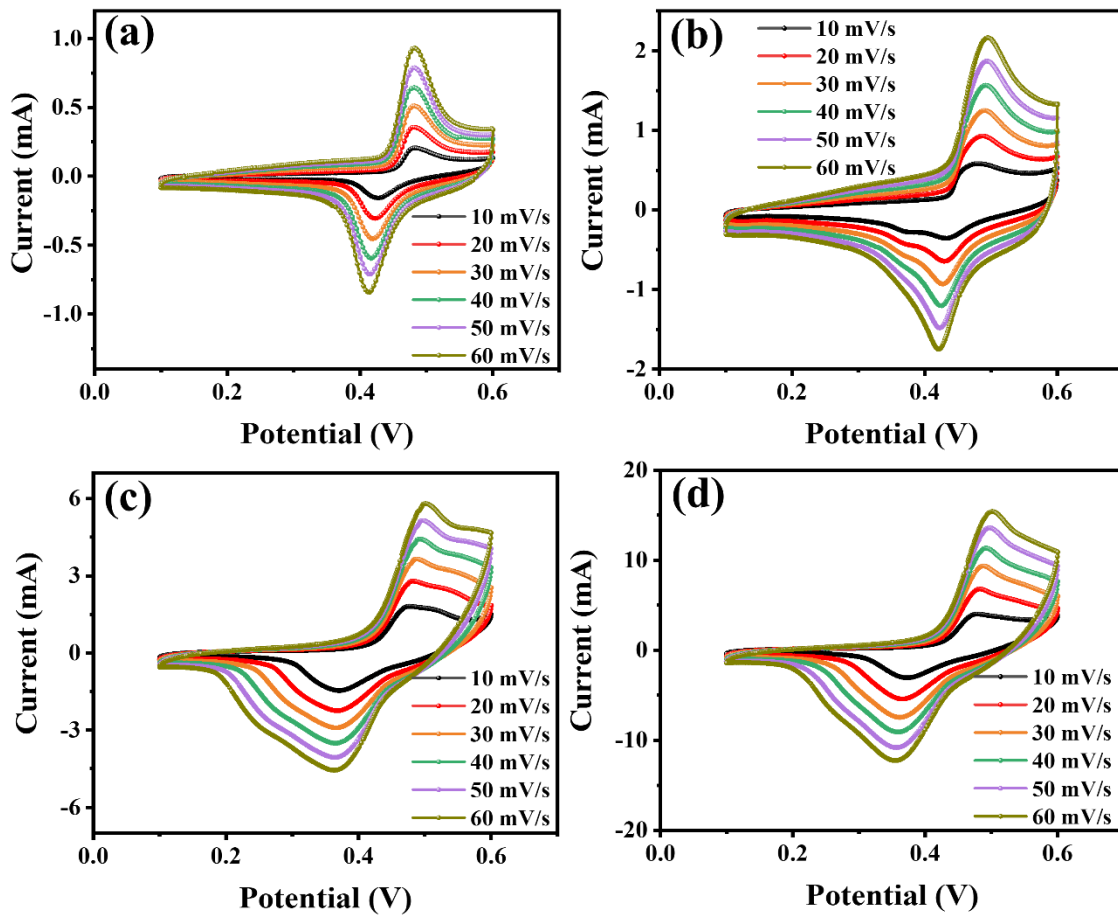


Figure S3 (a-d). Cyclic Voltammetry (CV) curves for the (a) pristine BNNT, (b) pristine ZnO, (c) BNNT-CNF hybrid and (d) BNNT-ZnO hybrid under various scan rates ranging from 10 mV/s to 60 mV/s in three electrode measurements.

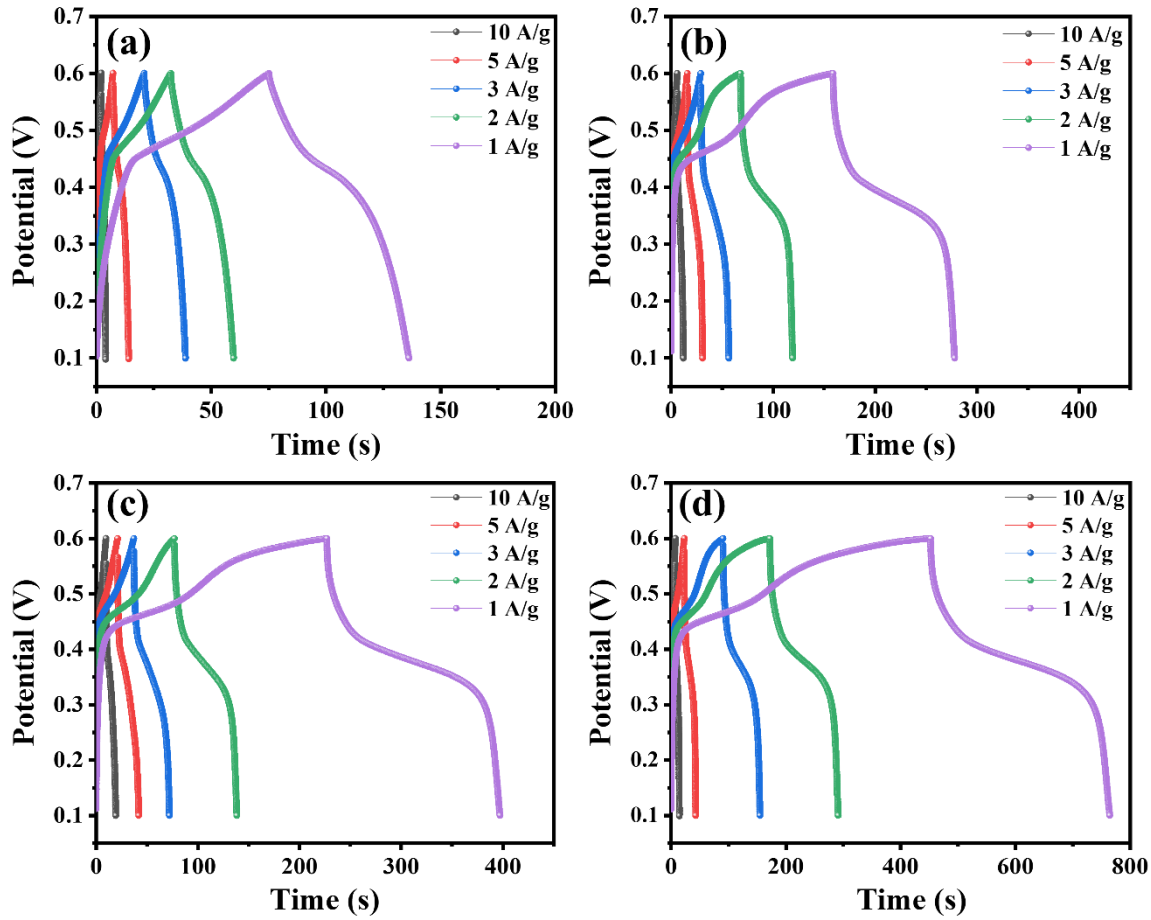


Figure S4 (a-d). Galvanostatic charging-discharging curves for the **(a)** pristine BNNT, **(b)** pristine ZnO, **(c)** BNNT-CNF hybrid and **(d)** BNNT-ZnO hybrid under various scan rates ranging from 10 mV/s to 60 mV/s in three electrode measurements.

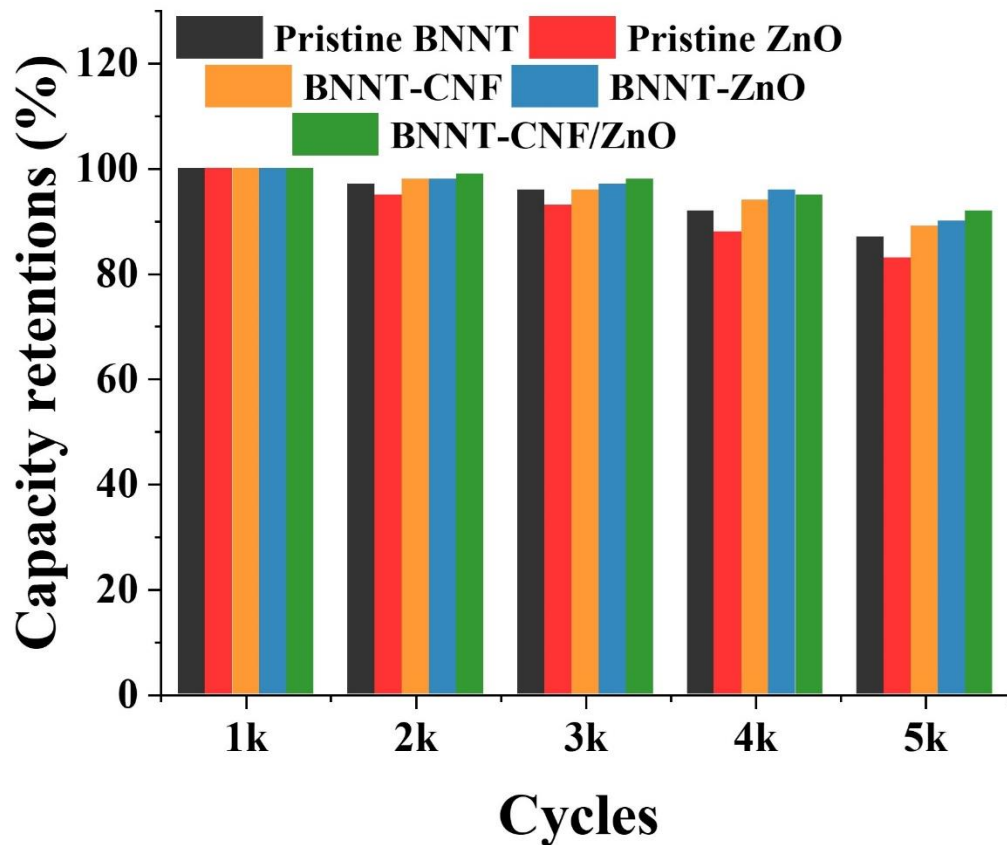


Figure S5. Cycling stability test under 5000 GCD cycles for the pristine BNNT, pristine ZnO, BNNT-CNF, BNNT-ZnO hybrid and BNNT-CNF/ZnO ternary nanostructure under 20 A/g of current density in a three electrode measurements.

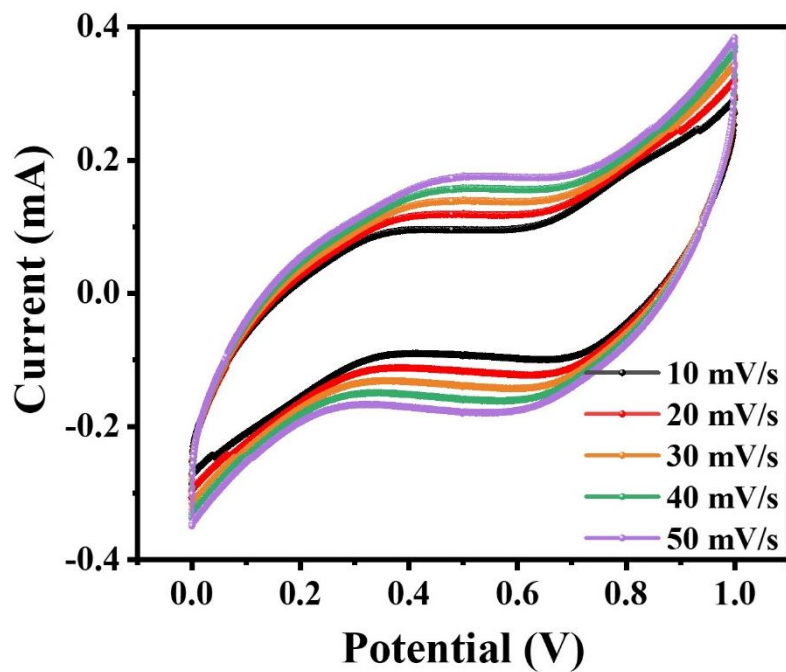


Figure S6. CV curves of BNNT-ZnO hybrid under various scan rates ranging from 10 mV/s to 50 mV/s in two electrode measurements.

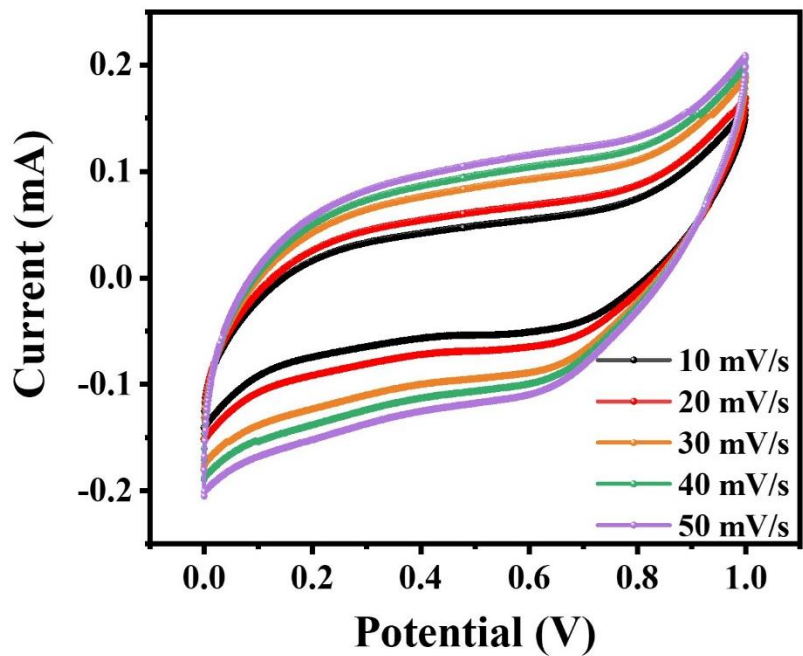


Figure S7. CV curves of BNNT-CNF hybrid under various scan rates ranging from 10 mV/s to 50 mV/s in two electrode measurements.

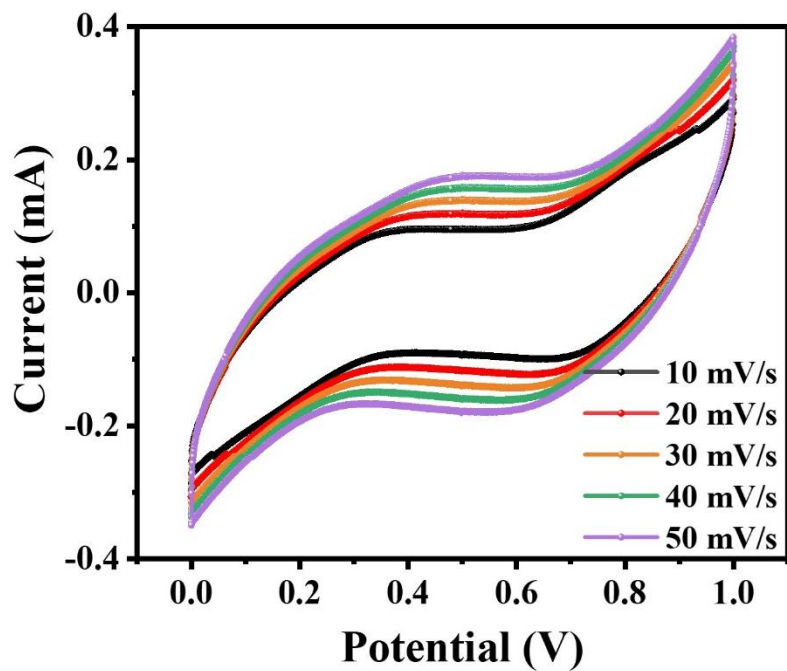


Figure S8. CV curves of pristine ZnO under various scan rates ranging from 10 mV/s to 50 mV/s in two electrode measurements.

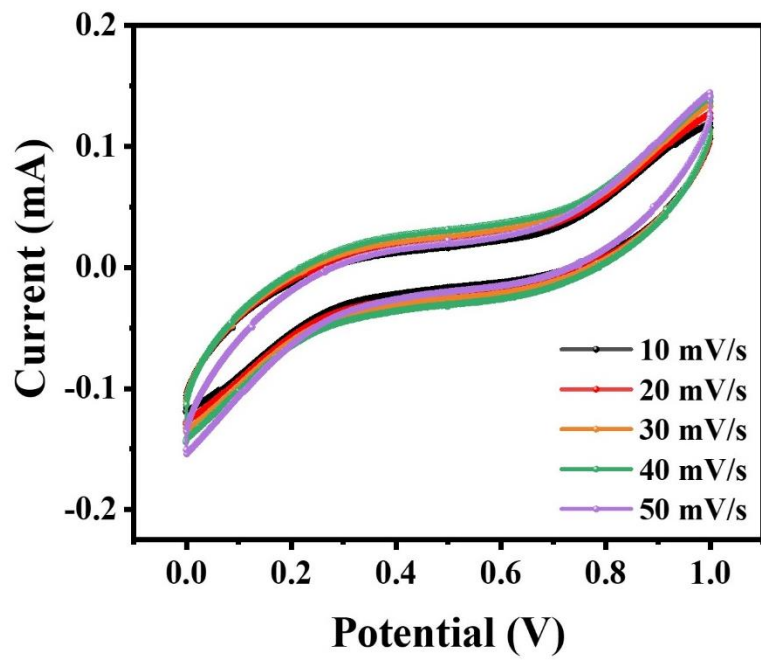


Figure S9. CV curves of pristine BNNT under various scan rates ranging from 10 mV/s to 50 mV/s in two electrode measurements.

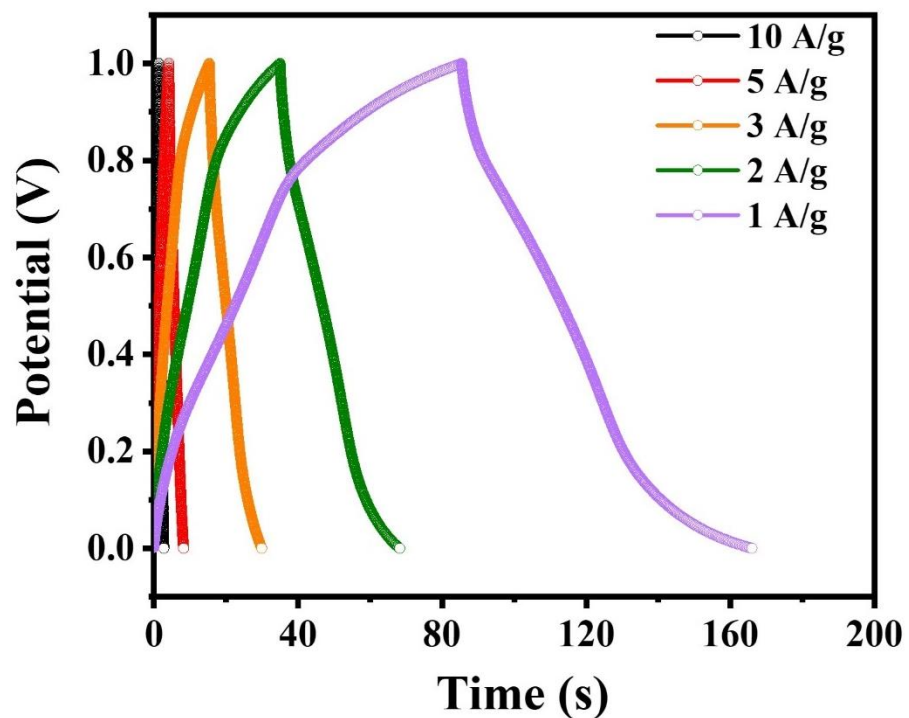


Figure S10. GCD curves of BNNT-ZnO hybrid under various current densities ranging from 1 A/g to 10 A/g in two electrode measurements.

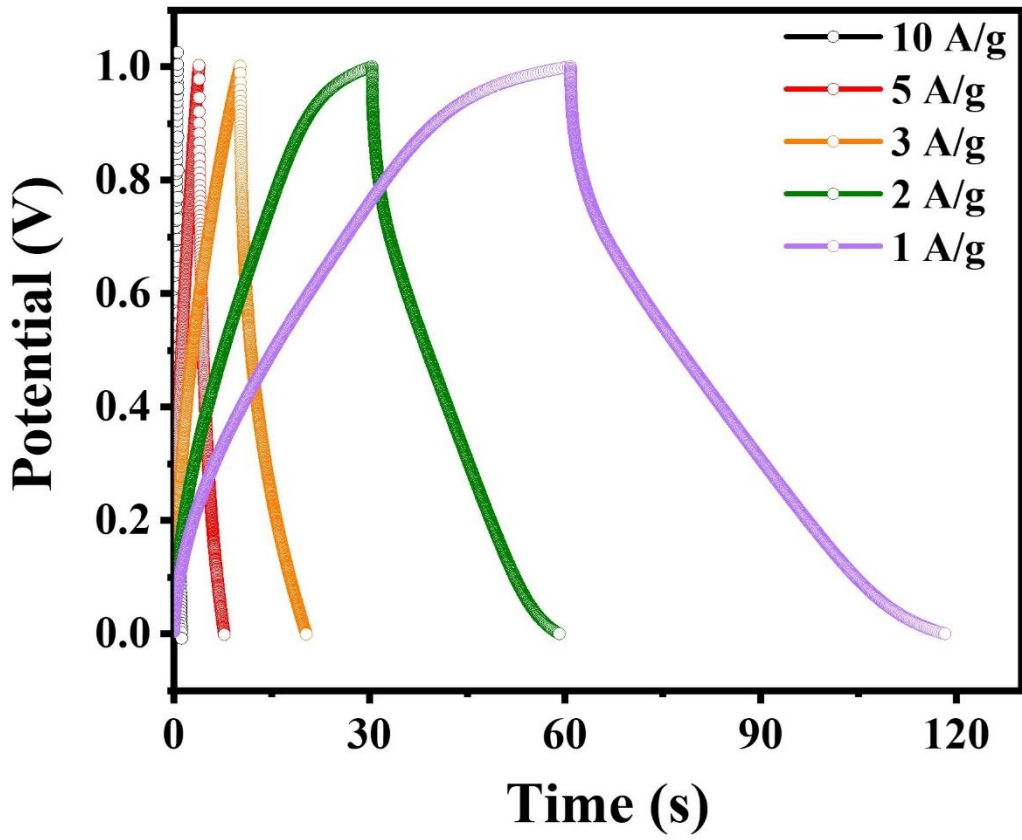


Figure S11. GCD curves of BNNT-CNF hybrid under various current densities ranging from 1 A/g to 10 A/g in two electrode measurements.

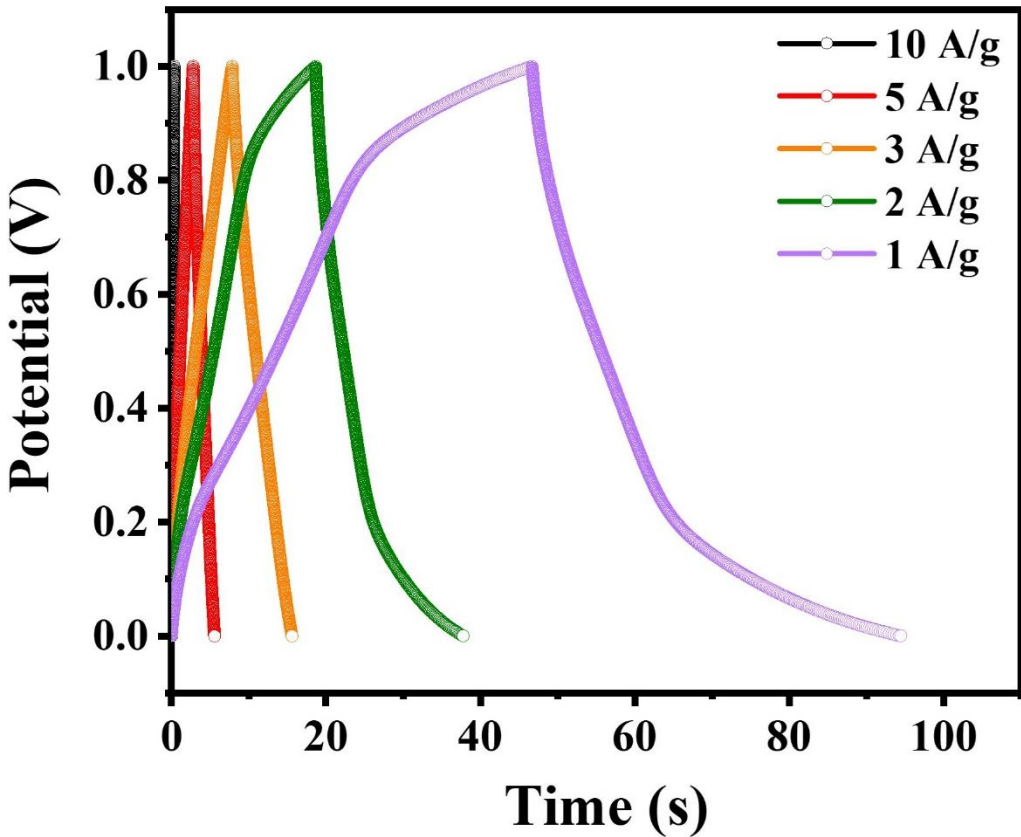


Figure S12. GCD curves of pristine ZnO under various current densities ranging from 1 A/g to 10 A/g in two electrode measurements.

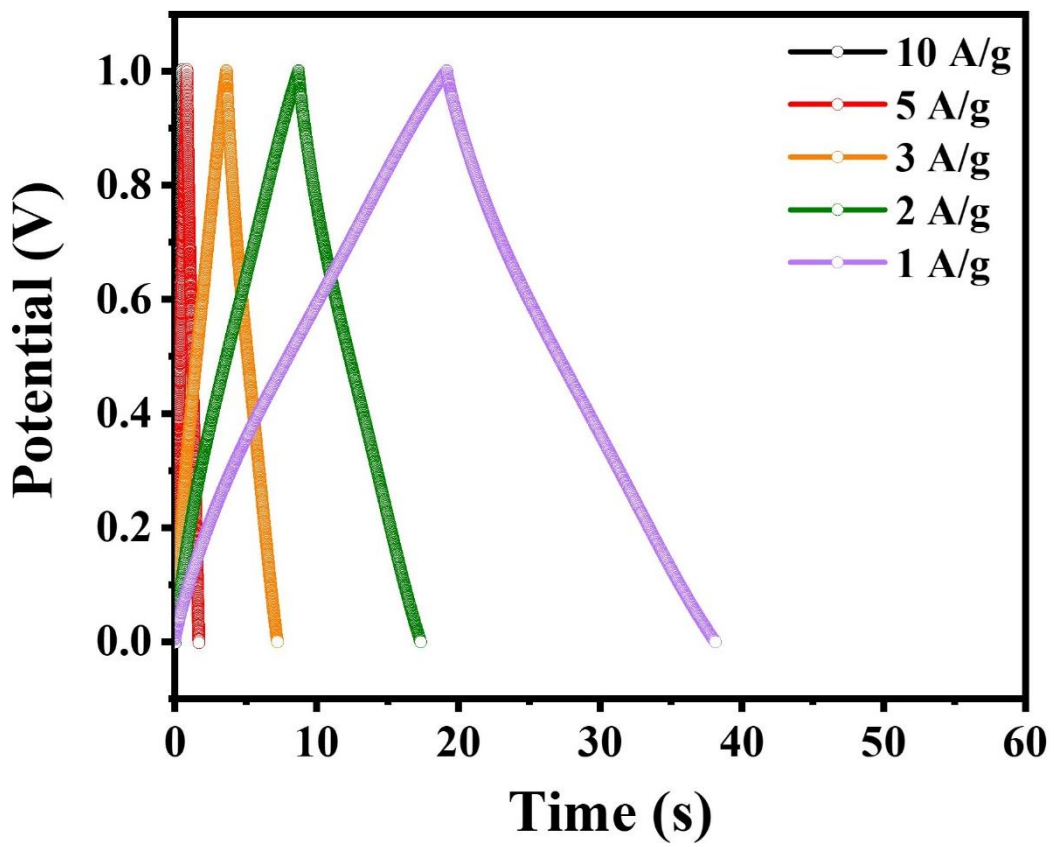


Figure S13. GCD curves of pristine BNNT under various current densities ranging from 1 A/g to 10 A/g in two electrode measurements.

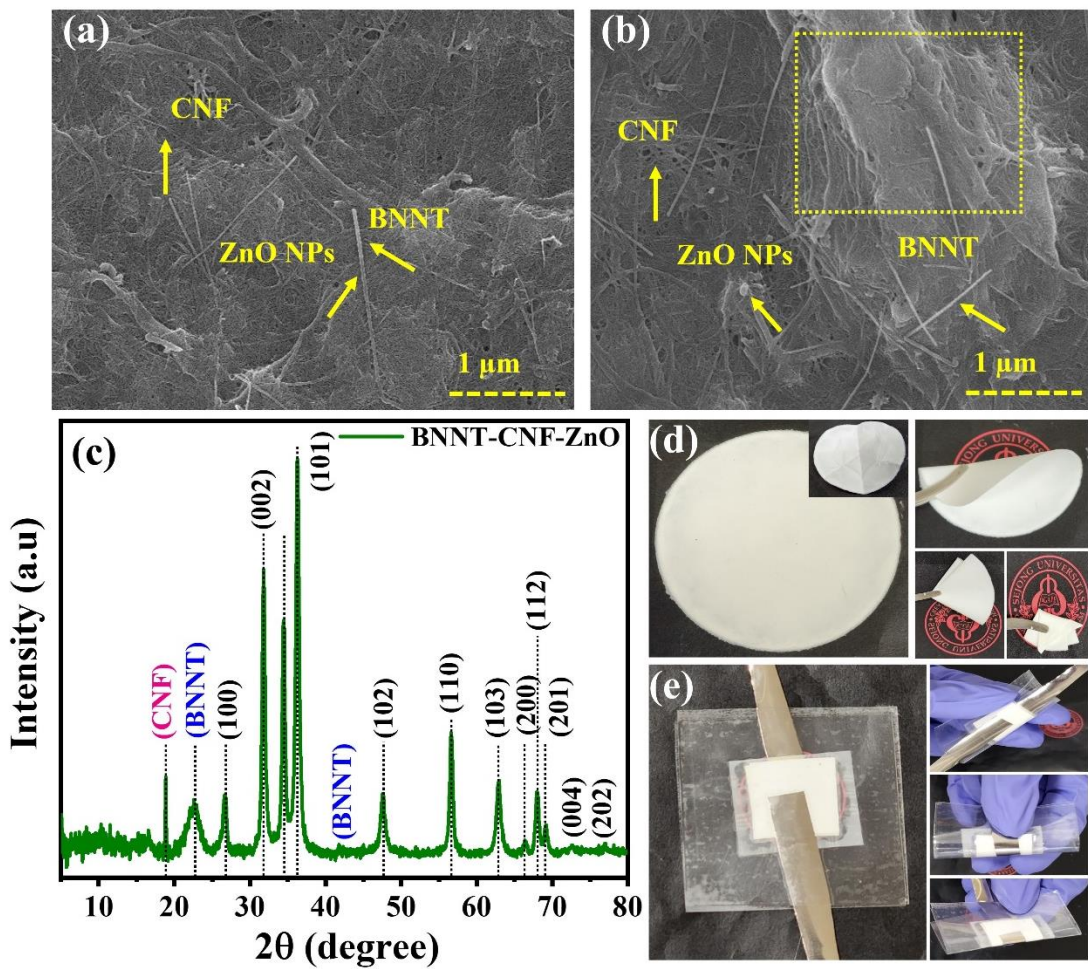


Figure S14. BNNT-CNF/ZnO ternary nanostructure paper performance such as **(a)** FESEM micrographs before cycling stability test, **(b)** after cycling stability (over 5000 cycles),and **(c)** XRD after cycling stability test. **(d)** Photo digital images for the BNNT-CNF/ZnO ternary nanostructure papers at different positions and **(e)** flexible symmetric supercapacitor device picture at different positions.

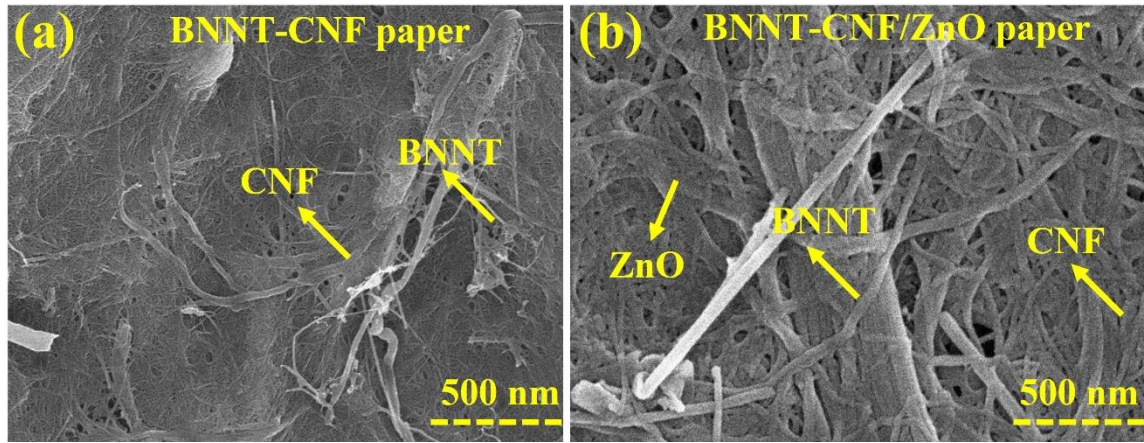


Figure S15. FESEM micrographs of the (a) BNNT-CNF and (b) BNNT-CNF/ZnO flexible paper.

Table S1. Comparative electrochemical performance of BNNT-CNF/ZnO in the three-electrode system with other previously reported materials.

Electrode materials	Electrolyte	Voltage window (V)	Capacitance (F/g) / Current density (A/g)	Ref.
BNNT-CNF/ZnO	3 M KOH	0.1 to 0.6	968 / 1	Present work
Co ₃ O ₄ @CNF	3 M KOH	-0.2 to 0.6	789.9 / 1	¹
ZnMn ₂ O ₄ /C	6 M KOH	0 to 1.2	589 / 1	²
ZnO/MnO ₂ nanowires	1 M Na ₂ SO ₄	0 to 0.9	501 / 2	³
ZnMn ₂ O ₄ /carbon	6 M KOH	-1 to -0.3	105 / 0.3	⁴
ZnO nanocones	1 M KOH	0.1 to 0.6	236 / 1	⁵
NCA/Co ₃ O ₄	6 M KOH	-0.05 to 0.45	616 / 1.2	⁶
CuCo ₂ S ₄ /CNT/graphe ne	1 M Na ₂ SO ₄	0 to 0.6	504 / 10 /	⁷
CPSC-3rGO	0.2 M Na ₂ SO ₄	-0.2 to 0.8	446 / 1	⁸
CS@ZnO Core-shell	6 M KOH	0 to 0.4	630 / 2	⁹
Co ₃ O ₄ nanoflakes@SrGO	2 M KOH	-0.2 to 0.5	406 / 1	¹⁰
CoMoO ₄ nanoclusters	6.0 M KNO ₃	-0.9 to 0.6	367 / 1.2	¹¹
ZnO-/core like MnO ₂	1 M Na ₂ SO ₄	0-0.8	221 / 0.5	¹²
Ni-Co selenide	6 M KOH	0 to 0.6	742.4 /1	¹³
ZnO/MnO ₂	0.5 M Na ₂ SO ₄	0 to 0.8	262 / 0.2	¹⁴

Table S2. Comparative electrochemical performance of BNNT-CNF/ZnO in all solid state symmetric/Asymmetric supercapacitor devices with other previously reported materials.

Electrode materials	Type	Electrolyte	Capacitance (F/g) / Current density (A/g)	Capacitance retention (%) / cycles	Ref.
BNNT-CNF/ZnO	Symmetric	PVA-KOH solid gel	300 / 1	96 / 5000	Present work
Co ₃ O ₄ @CNF	Symmetric	PVA-KOH gel	214 / 1.0	94 / 5000	¹
NCOs	Symmetric	1.0 M KOH	89 / 0.23	-	¹⁵
CNF-RGO	Symmetric	H ₂ SO ₄ -PVA	203 / 0.7	99 / 5000	¹⁶
1D-CoSe ₂ nanoarrays	Symmetric	PVA-KOH	152 / 0.5	96.8 / 5000	
ZnO/Co ₃ O ₄ -450//AC	Asymmetric	1.0 M KOH	153 / 1	-	¹⁷
CC@NiC ₂ O ₄ //CC@NC	Asymmetric	6.0 M KOH	89.7 / 1	86.7 / 20000	¹⁸
Co ₃ O ₄ @Ni ₃ S ₂	Asymmetric	3.0 M KOH	126 / 1	83.5 / 5000	¹⁹
Co ₃ O ₄ @Ni(OH) ₂ /AC	Asymmetric	6.0 M KOH	110 / 2.5	86 / 1000	²⁰
3D graphene-MoS ₂ hybrid	Symmetric	KOH/PVA	58.0 / 2	-	²¹
MoS ₂ -NH ₂ /PANI nanosheets	Symmetric	1 M H ₂ SO ₄	58.6 / 2	96.5 / 10000	²²
MoS ₂ /CNS	Symmetric	1 M Na ₂ SO ₄	108 / 1	-	²³

MoS ₂ /G nanobelts	Symmetric	1 M Na ₂ SO ₄	278.2 / 0.8	-	²⁴
MoS ₂ /rGO	Symmetric	1 M H ₂ SO ₄	306 / 0.5	-	²⁵
NiS/MoS ₂ @N-rGO	Symmetric	6 M KOH	1028 / 1	94.5 / 50000	²⁶
VSL-MoS ₂ @3D-Ni foam	Symmetric	Na ₂ SO ₄ /PVA	34.1 / 1.3	82.5 / 10000	²⁷
MoS ₂ /rGO	Symmetric	NaOH	323 / 0.2	76.8 / 500	²⁸
SS/MWCNTs/MoTe ₂	Symmetric	PVA-LiClO ₄	68.01 / 0.2	94 / 2000	²⁹
MWCNTs/MoSe ₂	Symmetric	PVA-KOH	27 / 0.4	95 / 1000	³⁰

Reference:

- I. Rabani, J. Yoo, H.-S. Kim, S. Hussain, K. Karuppasamy and Y.-S. Seo, *Nanoscale*, 2021, **13**, 355-370.
- Z. Zhu, Z. Wang, Z. Yan, R. Zhou, Z. Wang and C. Chen, *Ceramics International*, 2018, **44**, 20163-20169.
- S. Li, J. Wen, X. Mo, H. Long, H. Wang, J. Wang and G. Fang, *Journal of Power Sources*, 2014, **256**, 206-211.
- C.-K. Sim, S. R. Majid and N. Z. Mahmood, *Journal of Alloys and Compounds*, 2019, **803**, 424-433.
- X. He, J. E. Yoo, M. H. Lee and J. Bae, *Nanotechnology*, 2017, **28**, 245402.
- G. Sun, L. Ma, J. Ran, X. Shen and H. Tong, *Journal of Materials Chemistry A*, 2016, **4**, 9542-9554.

7. N. I. Chandrasekaran, H. Muthukumar, A. D. Sekar, A. Pugazhendhi and M. J. J. o. M. L. Manickam, 2018, **266**, 649-657.
8. J. S. Lee, C. Lee, J. Jun, D. H. Shin and J. Jang, *Journal of Materials Chemistry A*, 2014, **2**, 11922-11929.
9. X. Xiao, B. Han, G. Chen, L. Wang and Y. Wang, *Scientific reports*, 2017, **7**, 1-13.
10. M. Qorbani, T.-c. Chou, Y.-H. Lee, S. Samireddi, N. Naseri, A. Ganguly, A. Esfandiar, C.-H. Wang, L.-C. Chen and K.-H. Chen, *Journal of Materials Chemistry A*, 2017, **5**, 12569-12577.
11. J. Li, C. Zhao, Y. Yang, C. Li, T. Hollenkamp, N. Burke, Z.-Y. Hu, G. Van Tendeloo and W. Chen, *Journal of Alloys and Compounds*, 2019, **810**, 151841.
12. Y. Zhao, P. Jiang and S.-S. Xie, *Journal of power sources*, 2013, **239**, 393-398.
13. Y. Wang, W. Zhang, X. Guo, K. Jin, Z. Chen, Y. Liu, L. Yin, L. Li, K. Yin and L. Sun, *ACS applied materials & interfaces*, 2019, **11**, 7946-7953.
14. W. Li, G. He, J. Shao, Q. Liu, K. Xu, J. Hu and I. P. Parkin, *Electrochimica Acta*, 2015, **186**, 1-6.
15. X. Lu, X. Huang, S. Xie, T. Zhai, C. Wang, P. Zhang, M. Yu, W. Li, C. Liang and Y. Tong, *Journal of Materials Chemistry*, 2012, **22**, 13357-13364.
16. K. Gao, Z. Shao, J. Li, X. Wang, X. Peng, W. Wang and F. Wang, *Journal of Materials Chemistry A*, 2013, **1**, 63-67.
17. M. Gao, W.-K. Wang, Q. Rong, J. Jiang, Y.-J. Zhang and H.-Q. Yu, *ACS applied materials & interfaces*, 2018, **10**, 23163-23173.
18. C. Guan, X. Liu, W. Ren, X. Li, C. Cheng and J. Wang, *Advanced Energy Materials*, 2017, **7**, 1602391.

19. J. Zhang, J. Lin, J. Wu, R. Xu, M. Lai, C. Gong, X. Chen and P. Zhou, *Electrochimica Acta*, 2016, **207**, 87-96.
20. C.-h. Tang, X. Yin and H. Gong, *ACS applied materials & interfaces*, 2013, **5**, 10574-10582.
21. K. Singh, S. Kumar, K. Agarwal, K. Soni, V. R. Gedela and K. Ghosh, *Scientific reports*, 2017, **7**, 1-12.
22. R. Zeng, Z. Li, L. Li, Y. Li, J. Huang, Y. Xiao, K. Yuan and Y. Chen, *ACS Sustainable Chemistry & Engineering*, 2019, **7**, 11540-11549.
23. T. N. Khawula, K. Raju, P. J. Franklyn, I. Sigalas and K. I. Ozoemena, *Journal of Materials Chemistry A*, 2016, **4**, 6411-6425.
24. Y. Jia, H. Wan, L. Chen, H. Zhou and J. Chen, *Journal of Power Sources*, 2017, **354**, 1-9.
25. H. Ji, S. Hu, Z. Jiang, S. Shi, W. Hou and G. Yang, *Electrochimica Acta*, 2019, **299**, 143-151.
26. X. Xu, W. Zhong, X. Zhang, J. Dou, Z. Xiong, Y. Sun, T. Wang and Y. Du, *Journal of colloid and interface science*, 2019, **543**, 147-155.
27. R. K. Mishra, A. K. Kushwaha, S. Kim, S. G. Seo and S. H. Jin, *Current Applied Physics*, 2019, **19**, 1-7.
28. T. Xue, Y. Yang, X.-H. Yan, Z.-L. Zou, F. Han and Z. Yang, *Materials Research Express*, 2019, **6**, 095029.
29. S. S. Karade and B. R. Sankapal, *ACS Sustainable Chemistry & Engineering*, 2018, **6**, 15072-15082.
30. S. S. Karade and B. R. Sankapal, *Journal of Electroanalytical Chemistry*, 2017, **802**, 131-138.

